Energy Equilibration among the Chlorophylls in the Electron-Transfer System of Photosystem I Reaction Center from Spinach†

Shigeichi Kumazaki,*,‡ Isamu Ikegami,§ Hiroko Furusawa,‡ and Keitaro Yoshihara‡

School of Materials Sciences, Japan Advanced Institute of Science and Technology, Tatsunokuchi, Ishikawa 923-1292, Japan, and Faculty of Pharmaceutical Sciences, Teikyo University, Sagamiko, Kanagawa, 199-0195, Japan

Received: July 16, 2002; In Final Form: October 30, 2002

Excitation-wavelength dependence of the transient absorbance changes of photosystem I reaction center particles with a reduced number of antenna chlorophylls (16 chlorophylls/primary electron donor chlorophyll (P700)) has been studied in an effort to understand the energy equilibration among the chlorophylls in the electron-transfer system. The photobleaching and stimulated-emission signals in the Q_y band region of the chlorophylls upon the preferential excitation of chlorophyll spectral forms at the blue edge (662 nm) and red edge (697 nm) of the Q_y band are analyzed. In the case of the red-edge excitation, spectral equilibration proceeds with a time constant of 0.34 (±0.07) ps, which is attributable to the energy equilibration between P700 and neighboring chlorophylls absorbing around 686 nm in the electron-transfer system. This equilibration seems to precede the fastest phase of the primary charge separation (apparent time constant of 0.8 ps) reported previously (Kumazaki et al. *J. Phys. Chem. B* **2001**, *105*, 1093). A slow decay of the excited states because of the slow phase of the primary charge separation proceeds with a time constant of 7.2 (±0.6) ps. In the case of the blue-edge excitation, vibrational relaxation and downhill energy transfer proceed with a time constant of 0.38 (±0.08) ps, which are followed by a slow downhill energy transfer from residual antenna chlorophylls to the electron-transfer system. Even with the slow energy transfer from the residual antenna chlorophylls to the electron-transfer system, the overall primary charge separation is completed with a time constant of 10 (±0.7) ps. These interpretations are in part supported by control experiments on chlorophyll *a* in ethanol under equivalent optical conditions. Implications of these results for understanding the primary processes in more intact photosystem I are discussed.

1. Introduction

Photosystem I reaction center (PSI RC) pigment−protein complex, which is embedded in the thylakoid membrane of oxygenic photosynthetic organisms, utilizes light energy to transport electrons from reduced plastocyanin or cytochrome c_6 to soluble ferredoxin.[1] The core part of the PSI RC complex contains about 100 chlorophylls (Chls), several of which undergo the primary electron-transfer steps starting from excited states of Chls. The most recent X-ray analysis of the crystal structure of cyanobacterial PSI RC has shown the arrangement of the chlorophyll (Chl) molecules in the electron-transfer system (ETS) (reaction center, Figure 1).[2,3]

The energy transfer and primary charge separation in PSI RC has been extensively studied by time-resolved spectroscopy.[4−7] Upon photoexcitation of the antenna Chls, excitation migrates over several neighboring Chls on a time scale of 0.36−0.5 ps, which results in energy equilibration among major spectral types of bulk antenna Chls.[8−10] There are very often minor spectral forms of Chls that are called long-wavelength-absorbing Chls with their absorption peaks even redder than that of the electron

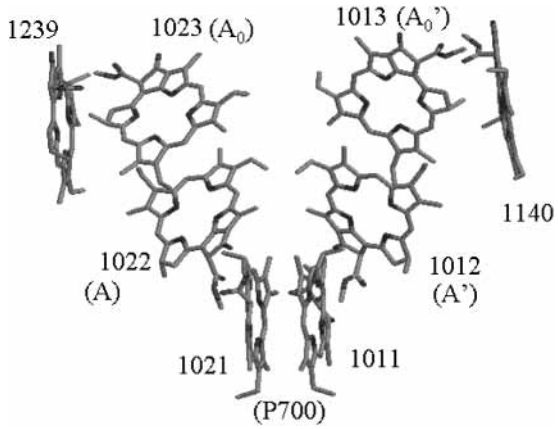

Figure 1. Arrangement of the six chlorophyll molecules in the electron-transfer system (1011−1013 and 1021−1023) of photosystem I from the cyanobacterium *Synechococcus elongatus*.[2,3] The molecular identity numbers are according to the file in the Protein Data Bank (1JB0). The two chlorophyll molecules, 1239 and 1140, are expected to mediate excitation energy transfer between the core antenna chlorophylls and the electron-transfer system. The pair of Chls, 1011 and 1021, probably corresponds to the electron donor chlorophyll (P700). The electron transfer from the excited state of P700 proceeds through 1022−1023 and/or 1012−1013 branch(es) to the phylloquinone acceptor(s) (not shown). It should be noted that the correspondence between the spectroscopic notations (P700, *A*, A_0, *A*′, A_0′), and the molecular identity numbers is not necessarily decided.

† Part of the special issue "George S. Hammond & Michael Kasha Festschrift".

* To whom correspondence should be addressed. E-mail: kumazaki@jaist.ac.jp. Phone: 81-(0)761-51-1523. Fax: 81-(0)761-51-1149.

‡ Japan Advanced Institute of Science and Technology.

§ Teikyo University.

10.1021/jp026532e CCC: $25.00
Published on Web 12/20/2002

donor Chl (P700). In such cases, the subpicosecond equilibration is followed by more extensive energy equilibration between the bulk antenna and the long-wavelength-absorbing Chls with typical time constants of 4−12 ps.[5] The major trapping of excitation energy due to the charge separation proceeds on a slower time scale (typically 20−50 ps) than the energy equilibration time scale. It should be, however, noted that minor nonequilibrium trapping proceeds on a similar time scale to that of the energy equilibration in some cases.[10,11]

One interesting issue that remains to be clarified is how energy is transferred between the core antenna Chls and P700. The two Chls (1239 and 1140 in Figure 1) located between the core antenna and the electron acceptor Chls, which are designated as "connecting Chls", have been assumed to mediate energy transfer between the core antenna and the ETS.[3] One recent study has shown that the excited-state lifetime of the antenna Chl can be dramatically elongated in a mutant RC that lacks these two Chls.[12] It is thus likely that the chains of Chls in the ETS are also working as the channel for the energy transfer between P700 and the core antenna Chls. It is then intriguing to characterize the spectral properties and the energy transfer processes associated with the ETS Chls. This is, however, an extremely difficult task, because there are typically ≈ 90 core antenna Chls which mask the energy transfer steps.[2,3]

By the diethyl ether treatment of spinach PSI RC, all of the carotenoid and secondary acceptor phylloquinone and about 90% of Chls can be removed in order to yield PSI RC containing as few as 9 Chls per P700.[13,14] Such a preparation of PSI RC, which is designated as P700-enriched RC, shows the electron transfer to the acceptor Chl, A_0, because the acceptor phylloquinone is absent.[15,16] The electron transfer to the first iron−sulfur center, F_X, is fully recovered when phylloquinone or analogous quinone is reconstituted.[16−18] The characterization of the electron transfers in the P700-enriched RC has played a leading role for the understanding of the primary charge separation and the subsequent electron-transfer steps in intact PSI RC.[4,6,14,17]

The high ratio of the ETS Chls in the P700-enriched RC should help one to characterize the spectral properties of the ETS Chls and how energy is transferred among them. It is especially desirable to understand the dependence of the energy transfer on excitation wavelength. The excitation at the red-edge (e.g., 700 nm) of the Qy band of the P700-enriched RC actually has manifested an ultrafast phase of the primary charge separation (0.8 ps)[19] that has never been observed with excitation at shorter wavelengths.[15,20] However, the excitation wavelength dependence of the primary photochemistry has not been systematically investigated under rigorously the same optical setup in the case of the P700-enriched RC.

In this study, we have applied femtosecond transient absorption spectroscopy to the P700-enriched RC particles with about 16 Chls/P700. The excitation wavelength was selected at the blue edge or red edge of the Qy band of the Chls, and the photobleaching and/or stimulated emission of the Qy band was observed in order to differentiate the spectral forms of Chls. The excitation-wavelength dependence is expected to reveal the spatial arrangement of different spectral forms of Chls.[21] As a control experiment, we have also performed the transient absorption measurement on Chl *a* in ethanol under equivalent optical conditions, by which we are rigorously able to distinguish intermolecular transfer processes among Chls in P700-enriched RC from relaxation processes of individual monomer Chls. A preliminary account of some part of this work was presented at the XIth International Photosynthesis Congress, August 1998, in Budapest.[22]

2. Materials and Methods

The P700-enriched RC particles were prepared as previously reported.[13,14,23] In brief, the lyophilized spinach PS I particles obtained by a digitonin treatment were extracted twice with diethyl ether containing water at 80% saturation. They were solubilized by incubation for 30 min with 20 mM phosphate buffer (pH 8) containing 0.2% Triton X-100. The insoluble, grayish-white material was removed by centrifugation. The blue-green supernatant, which had a chlorophyll/P700 ratio of about 16, was used as P700-enriched RC, unless otherwise mentioned. In a limited experiment, P700-enriched RC with about 12−13 Chl was used. Ascorbate and 2,6-dichlorophenolindophenol were added to final concentrations of 7 mM and 70 μM, respectively, to prepare the RC particles under the P700-neutral conditions. The temperature of the sample was maintained at 0−5 °C during all of the treatments to minimize damage of the samples.

The transient absorbance changes were determined by comparing the transmission of the probe pulse through the samples between pump-on and pump-off conditions. The pump pulses were taken from an optical parametric amplifier (OPA), which were operated by a femtosecond Ti:sapphire oscillator-amplifier system. Their spectra are shown in Figures 2a and 6a. The pump pulses were sent through a computer-controlled delay optics to the sample. Two different optical and data-acquisition schemes were used. In the first scheme (transient spectrum method), femtosecond white continuum pulses generated by the amplified 800 nm pulses were used to probe the absorbance changes over the 654−716 nm region. A dual photodiode array detector attached to an exit port of a monochromator was used. One array monitored the probe pulse spectrum after transmission through the sample that was irradiated by the pump beam, and the other monitored the fluctuation of the probe pulse spectrum without transmission through the sample. In the second scheme (single wavelength method), another OPA generated probe pulses, the spectra of which were limited by interference filters to a full width at half-maximum (fwhm) of 12 nm. In this case, a mechanical chopper at the half of the repetition rate of the pulses (500 Hz) modulated the pump beam with a fixed phase to the pulse train. One photodiode detector was used to monitor the probe pulse energy after transmission through the sample that was irradiated by the pump beam, and the other monitored the fluctuation of the probe pulse energy without transmission through the sample. The pulse energies were recorded at 1 kHz. The instrument-response function (IRF) at each probe wavelength was determined by the sum-frequency cross correlation between the pump and probe pulses in a BBO crystal of a 0.3 mm thickness. The zero time was defined to be the peak of the IRF. The fwhm of the IRF was 0.19−0.22 ps in the single wavelength method and 0.31−0.35 ps (depending on the probe wavelength) in the transient spectrum method. The angle between the pump and probe polarizations was set at the magic angle (54.7°).

The sample was put in a cylindrical cuvette with a path length of 1.5 (±0.1) mm. Two microscopic cover glasses with a thickness of 0.17−0.25 mm were used as the optical windows of the cell. This cuvette was cooled (≈280 K) and rotated at a sufficient speed during the measurements to ensure that each pair of the pump−probe pulses would irradiate a new portion of the sample. The absorbance at the Q_y band peak was 0.9−1.1 for the 1.5 mm path length. The peak wavelength was checked before and after each measurement, and the change was at most 1.0 nm. The energies of the pump and probe pulses were 40−50 nJ and <10 nJ, respectively. The diameters of the pump and probe beams at the sample positions were 0.3 and

0.15 mm, respectively. Under these conditions, the maximum photobleaching signal in the Q_y band region was −0.010 (±0.002) in the absorbance scale. We estimated that at most 15% of the RC particles were excited by each pump pulse.

Chl *a* of *Chlorella* was purchased from Wako Pure Chemical Industries, Ltd. and used as received. For the preparation of Chl *a* in ethanol, spectroscopic grade ethanol was used as the solvent. The concentration of Chl *a* was adjusted so that the absorbance at the peak of the Q_y band was 0.7−0.8 for the 1.5 mm optical path, where there was no indication of aggregate formation.

3. Results

Figure 2, parts b and c, shows the transient absorption spectra at three representative delay times (0.3, 2.0, and 18 ps) upon the 697 and 662 nm excitations, respectively. The peak of photobleaching plus stimulated emission signal (PB/SE signal) in the 0.3 ps spectrum upon the 697 nm excitation is at 691 nm, which is significantly red-shifted than the one (680 nm) upon the 662 nm excitation. From 0.3 to 2 ps after the 697 nm excitation, the total PB/SE signal seems to shrink and shifts its weight to the bluer wavelength region. The spectral shape at 18 ps (Figure 2d) is similar to that of the radical pair spectrum of $P700^+A_0^-/P700A_0$, which has been obtained by nanosecond flash photolysis for the P700-enriched RC.[18] On the other hand, the PB/SE signal upon the excitation at 662 nm gradually shifts to the red from 0.3 to 18 ps. Between the transient spectra at 18 ps with the different excitation wavelength at 662 and 697 nm, there is a high similarity in the wavelength region between 690 and 710 nm, but there is a clear difference in the wavelength region between 670 and 690 nm (Figure 2d).

The transient absorption data sets as in Figure 2, parts b and c, were analyzed by the global curve fitting analysis. The data later than 0.2 ps were fitted by the sum of two exponential functions, because IRF-limited appearance of signals were found to be completed at 0.2 ps (see the Materials and Methods section). The analysis yielded time constants of 0.34 and 7.2 ps for the 697 nm pump conditions, and 0.38 and 10 ps for the 662 nm pump conditions, as in Table 1. The plot of the amplitudes that decay with a common time constant against wavelength is called decay-associated spectrum (DAS), which is shown in Figure 3 for each time constant and excitation wavelength.

For the special interest in the spectrum of the excited state of P700 (P700*), Figure 4 shows the transient spectra at −0.1, +0.1, and +0.3 ps in the case of the excitation at 697 nm. The appearance of some signals at −0.1 ps is due to the definition of the zero time (see the Materials and Methods Section). The peak position shifts from 697 nm at −0.1 ps to 691 nm at 0.3 ps. The spectral width (fwhm) of the PB/SE signal broadens from 12 nm at −0.1 ps to 21 nm at 0.3 ps. It should be noted that the transient spectra earlier than 0.2 ps were not included in the above-mentioned global curve fitting.

The transient absorption signal at 699 nm is mainly given by the PB/SE signal of P700* and/or $P700^+$. The kinetic traces at 699 nm are shown in Figure 5 for the 697 and 662 nm excitation conditions. The kinetic trace with the 697 nm excitation shows an IRF-limited appearance of the PB/SE signal, and a subsequent decay within 1 ps after the excitation (Figure 5a). The transient absorbance change between 1 and 19 ps seems to be almost constant (Figure 5a). The signal at 699 nm upon the excitation at 662 nm rises within 1 ps to about 50% of the final nondecaying amplitude in this time window (Figure 3b and 5b). The remaining 50% of the final amplitude rises with a time constant of 10 ps (Figure 3b and 5b).

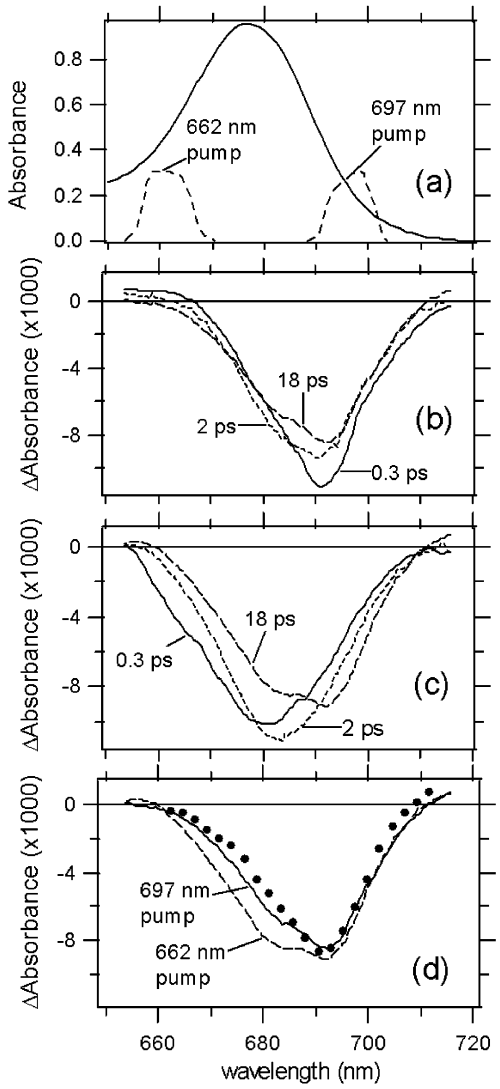

Figure 2. (a) Steady-state absorption spectrum of P700-enriched RC sample with a chlorophyll/P700 ratio of about 16 (solid line) together with the spectra of excitation pulses (broken lines). (b) Representative transient spectra upon the excitation at 697 nm. (c) Representative transient spectra upon the excitation at 662 nm. (d) Solid and broken lines represent the transient spectra at 18 ps upon the 697 and 662 nm excitations, respectively. Dots represent the radical pair spectrum of $P700^+A_0^-/P700A_0$ on a nanosecond time scale, which was reproduced from ref 18. For a systematic comparison between the two excitation conditions, all of the transient absorbance changes (in all figures) under the 662 nm excitation conditions were multiplied by a constant so that the 18 ps spectrum upon the 662 nm excitation shows the same amplitude at 700 nm as that upon the 697 nm excitation.

TABLE 1: Time Constants Obtained by the Transient Absorption Spectroscopy on P700-Enriched RCs

time constants (ps)	excitation (nm)	probe (nm)	chlorophyll /P700	ref
0.34 (±0.07)ps, 7.2 (±0.6) ps	697	654−716	16	this work
0.38 (±0.08) ps, 10 (±0.7) ps	662	654−716	16	this work
0.28 (±0.06) ps	699	700 (±6)	12−13	this work
8.4 ps	630	740 (±10)	12−13	20
0.8 ps (50%), 9 ps (50%)	699	738 (±10)	12−13	19

The transient absorbance changes of chlorophyll *a* in ethanol were analyzed by the global curve fitting. Only DAS are shown in Figure 6, parts b and c. With the red-edge excitation at 677

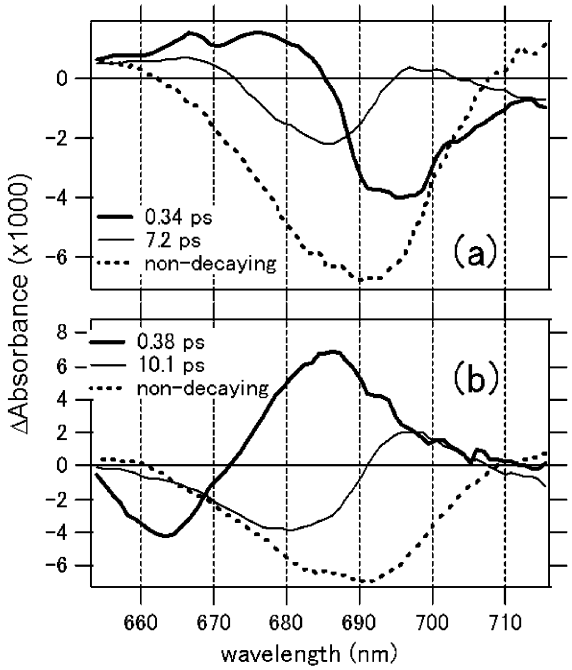

Figure 3. Decay-associated spectra obtained by the global analysis on the transient spectra at times later than 0.2 ps as shown in Figure 2. (a) under the 697 nm excitation conditions; (b) under the 662 nm excitation conditions.

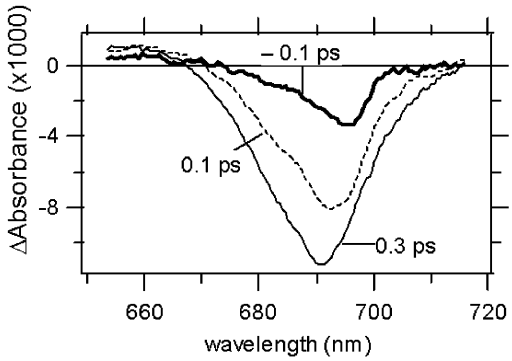

Figure 4. Transient absorption spectra at early delay times in the case of the 697 nm excitation. The spectra at −0.1 and +0.1 ps were not included as the target of the global curve fitting analysis.

nm, there is a component with a time constant of 1.1 ps (Figure 6 b). With the blue-edge excitation at 653 nm, there are two components with time constants of 0.16 and 0.64 ps (Figure 6c). The kinetic trace of the transient absorbance change at 681 nm upon the excitation at 677 nm is shown in Figure 7, where changes on a subpicosecond time scale is relatively small compared with that in the case of the P700-enriched RC upon the 697 nm excitation (Figure 5a).

4. Discussion

4.1. Distinction between Fast and Slow Energy Transfers in the P700-Enriched RC. There have been several works that reported excitation wavelength dependence of transient absorbance changes and/or of fluorescence spectrum changes of PS I RC core complex with about 100 Chls per P700.[8,24−26] One common result is that there is a so-called trapping component. This indicates excitation decay because of the charge separation after equilibration of excitation energy among the chlorophylls. It is characterized by a typical time constant of 20−50 ps and an associated DAS spectrum, which are almost independent of the excitation wavelength.

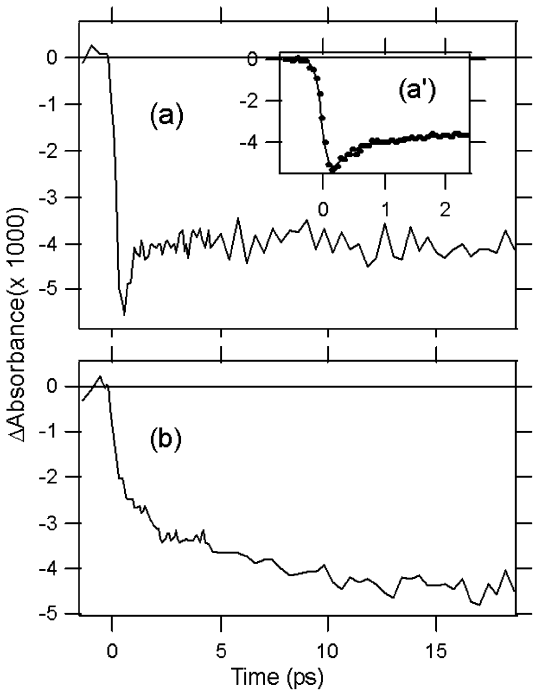

Figure 5. Plots of transient absorbance changes at 699 (±2) nm of the P700-enriched RC against time (lines connecting the data points). (a) Upon the 697 nm excitation, with 16 Chls/P700, by the transient spectrum method. The inserted graph (a′) shows the equivalent plot in a narrow time range obtained by the single wavelength method on P700-enriched RC with 12−13 Chl/P700. Dots represent the data, which were fitted by a convolution (solid line) between the instrument-response function and the sum of a double exponential function (with time constants of 0.28 (predominant amplitude) and 7.2 ps (small amplitude)) and a nondecaying component. (b) Upon the 662 nm excitation, with 16 Chls/P700, by the transient spectrum method.

In the case of the P700-enriched RC, there seems to be no equivalent trapping component that is common to the two excitation conditions (662 and 697 nm). Formation of the radical pair of chlorophylls at physiological temperatures is completed within 20 ps in the P700-enriched RCs with excitation wavelength at 630, 638, or 700 nm.[15,19,20] This indicates that the primary charge separation is completed with the time constant of 7.2−10 ps in this study. The spectral shape of the 7.2−10 ps DAS clearly depends on the excitation wavelength (Figure 3). The second time constant observed upon the 662 nm excitation (10 (±0.7) ps) is longer than that upon the 697 nm excitation (7.2 (±0.6) ps; Table 1). In the case of the excitation at 697 nm, a stationary PB/SE signal at 699 nm is observed after about 1 ps (Figure 5a). In the case of the 662 nm excitation, on the other hand, there is a continuous growth of the PB/SE signal up to 19 ps (Figure 5b). There is a substantial PB/SE signal below 670 nm within 2 ps upon excitation at 662 nm, whereas there is almost no PB/SE signal below 670 nm at all of the delay times upon the excitation at 697 nm. These indicate that there is a downhill energy transfer from Chls absorbing below 670 nm to lower-energy-lying Chls upon the 662 nm excitation on a picosecond time scale, but the reverse energy transfer to Chls absorbing below 670 nm is not observable upon the excitation at 697 nm.

The 0.34 ps DAS in the case of the excitation at 697 nm shows positive amplitudes below 675 nm. However, it is unlikely that there is a significant energy transfer on this time scale to Chls absorbing below 675 nm. This idea is supported as follows. First, the energy gap between Chls absorbing below 675 nm and Chls absorbing around 697 nm should be too large

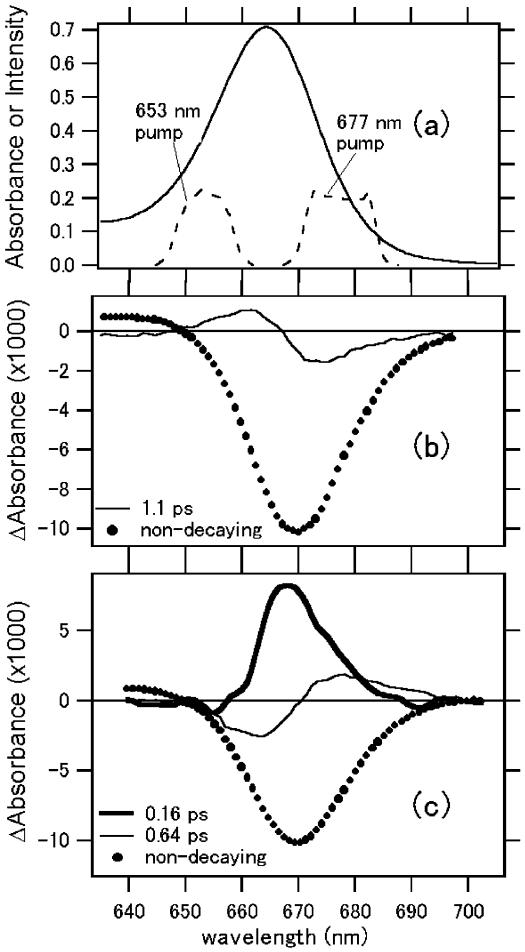

Figure 6. (a) Steady-state absorption spectrum of chlorophyll *a* in ethanol (solid line) and the spectra of excitation laser pulses (broken lines) centered at 653 nm and at 677 nm. (b and c) Decay-associated spectra obtained by the global analysis on the transient spectra of chlorophyll *a* in ethanol. (b) Under the 677 nm excitation conditions. (c) Under the 653 nm excitation conditions.

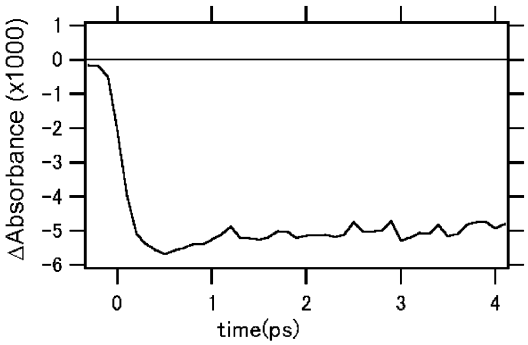

Figure 7. Kinetic trace of the transient absorbance change at 681 (±2) nm upon the excitation of chlorophyll *a* in ethanol at 677 nm. Transient spectrum method was used.

to allow a transfer time of 0.34 ps. Second, the PB/SE component in the 7.2 ps DAS in the case of the excitation at 697 nm should represent which Chl spectral forms are excited by the optical excitation at 697 nm and/or the subpicosecond uphill energy transfers. The PB/SE peak is located at 686 nm and there is no PB/SE signal below 673 nm. It is thus likely that the positive amplitude below 675 nm in the 0.34 ps DAS is given by the absorption of P700*. It should be noted that the excited-state absorption of P700 is far more intense than that of monomer Chl, at least around 720−750 nm.[19] In contrast, the positive amplitude between 685 and 675 nm in the 0.34 ps DAS is given by the appearance of the PB/SE signal of energy-accepting Chls.

TABLE 2: Tentative Estimation of the Time Constant of the Single Step Excitation Energy Transfer between Chl Pairs in the Electron-Transfer System, Two Connecting Chls, and Two Selected Core Antenna Chls

pair of molecules[a]	time constant[c] (ps)
1239−1238[b]	0.66
1023−1239	0.19
1022−1023	0.052
1021−1022	0.11
1011−1021	0.019
1012−1011	0.10
1013−1012	0.067
1140−1013	0.83
1139[b]−1140	0.74

[a] The identity numbers of the Chl are according to the Protein Data Bank file (photosystem I from *Synechococcus elongatus*, 1JB0). See Figure 1 and section 4.1 for the designation of the chlorophyll molecules. [b] The Chls designated as 1238 and 1139 are not shown in Figure 1. [c] The estimation is based on the Förster energy-transfer formula (note 28) and the Protein Data Bank file.

Although we do not yet exactly know which antenna Chls remain in the P700-enriched RC, it should be relatively difficult to extract chlorophylls in the central part of the PSI RC complex than Chls at the peripheral regions. We have tentatively estimated the time constants of the single-step energy transfers between the nearest neighbors of the ETS Chls (6 Chls) plus the two connecting Chls (1140 and 1239 in Figure 1) by the Förster energy-transfer formula on the basis of the crystal structure and some reasonable parameters (Figure 1).[27−29] Among these eight Chls, seven Chls are connected with single-step transfer times of less than 0.2 ps (Table 2). The shortest time constants of the energy transfer between the connecting Chls and the core antenna Chls in the crystal structure were also estimated to be 0.66 and 0.74 ps for the Chl pairs of 1239−1238 and 1139−1140, respectively (Table 2), which are at least three times longer than those among the above-mentioned seven Chls (Table 2). The 0.38 ps rise of the PB/SE signal of P700 upon the 662 nm excitation (Figure 3b) is thus attributable to the energy transfer from the seven Chls (actually including P700) to P700. It should be here noted that the 0.38 ps DAS does include energy transfers starting from residual antenna Chls. The residual core antenna Chls should then contribute to the 10 ps rise of the PB/SE signal of P700 upon the 662 nm excitation (Figure 3b).

The amplitude ratio between the 0.38 and 10 ps components at 699 nm is about 50:50 in Figure 3b, which is close to the ratio of the number of molecules (about 7:9) between the Chls in the ETS plus the one connecting Chl (the above-mentioned seven Chls) and the other Chls (about 9 Chls). If we consider the fact that one or two Chls are isolated from the ETS in terms of energy transfer (see section 4.4),[21] the amplitude ratio of 50:50 should be compared with the ratio of the number of molecules of 7:7 or 7:8. The probability of the direct excitation of P700 and A_0 in the ETS by the 662 nm excitation pulse are expected to be relatively low. These suggest that the whole set of the 6 Chls in the ETS as well as the connecting Chls are preserved in the P700-enriched RC. However, it should be noted that there may be structural differences between the PSI of spinach studied in this paper and of the cyanobacterium whose structure is known, although no discrepancy has been found between plant and cyanobacteria in terms of electron-transfer dynamics of PSI RC.

4.2. Equilibration of Excitation Energy Among the Chlorophylls in the Electron-Transfer System. The kinetic trace

of the transient absorbance change at 699 nm of the P700-enriched RC upon the excitation at 697 nm shows the decay of the PB/SE signal with the time constant of 0.34 ps (Figure 3a and 5a). In the case of Chl *a* in ethanol, there is a change in the transient spectrum with a time constant of 1.1 ps (Figure 6b and 7), which is attributable to a vibrational relaxation and/or solvent relaxation.[30] The 0.34 ps component of the P700-enriched RC is faster and more pronounced in amplitude than the 1.1 ps component of Chl *a* in ethanol. The 0.34 ps component should indicate intermolecular transfer processes. It should be mainly attributable mainly to energy transfer, not to electron transfer, for the following two reasons. First, the 7.2 ps component in the case of the 697 nm excitation of the P700-enriched RC shows a decay of PB/SE peaking around 686 nm (Figure 3a). This is a decay of Chl excited states that are generated by an uphill energy transfer from P700*, which should be achieved prior to the 7.2 ps decay. Second, our previous study has shown that the absorption of the Chl radical pair rises with two time constants of 0.8 (±0.1) (50%) and 9 (±1) ps (50%) in the P700-enriched RC with 12−13 Chls/P700 (Table 1).[19] The decay of PB/SE signal at 700 nm was also determined to be 0.28 (±0.05) ps in the case of the P700-enriched RC with 12−13 Chls/P700 in this study (Figure 5a′), which is in good agreement with the time constant of 0.34 (±0.07) ps in the case of 16 Chls/P700 (Figure 3a and 5a). These indicate that the 0.34 ps component is attributable mainly to energy equilibration starting from P700*.

The time constant of the uphill energy transfer from P700* upon the 697 nm excitation (0.34 ps) is similar to that (0.38 ps) of the downhill energy transfer upon the 662 nm excitation, which appears to be contrary to the detailed balance principle. However, the latter downhill energy transfer is not exactly the reverse process of the former uphill transfer. This primarily reflects the fact that the initial state in the case of the 662 nm excitation is actually a mixture of excited states of several Chls (including residual antenna Chls and ETS Chls), whereas the initial state in the case of the 697 nm excitation is almost exclusively P700*.

The PB/SE peak at 686 nm in the 7.2 ps DAS represents a decay of excited Chls due to a slow phase of the primary charge separation (Figure 3a and Table 1). The peak position at 686 nm is considerably more red-shifted than that (680 nm) of the 10 ps DAS in the case of the 662 nm excitation (Figure 3b). This suggests that excitation equilibration upon the 697 nm is limited to a subset of the Chls, which are presumably the Chls in the ETS.

The appearance of the bleaching of A_0 at 686 nm because of its reduction by the primary charge separation should be included in the 7.2 ps DAS.[16,31] This suggests that the true amplitude of the decay of PB/SE at 686 nm because of excited Chls is even larger than the apparent amplitude of the 7.2 ps DAS at 686 nm. The PB/SE signal at 686 nm seems to be relevant to the properties of the delayed fluorescence that was observed previously.[32] Because of the absence of the acceptor phylloquinone in the P700-enriched RC, the charge-separated state of $P700^+A_0^-$ generates the delayed fluorescence with a lifetime of 53 ns and a peak at 693 nm at 273 K.[32] Considering the typical Stokes shift of Chl *a* (5−6 nm) and the fluorescence peak of P700 in the P700-enriched RC (701 nm at 77 K),[14,21] the peak of the delayed fluorescence at 693 nm seems to be given by a mixture of P700* and a few Chls that shows the PB/SE peak around 686 nm. In other words, after the optical excitation of P700 at 697 nm, the spectral equilibration with a time constant of 0.34 ps prepares a mixture of excited states of P700 and a few neighboring Chls in the ETS, which are similar to those responsible for the delayed fluorescence.

The dynamics of the fluorescence anisotropy (at 749 nm) of the P700-enriched RC upon the 701 nm excitation was studied previously with an IRF of 0.45 ps.[33] The anisotropy was initially about 0.3, and it decayed to 0.15 with a time constant of 1.0 ps.[33] The spectral equilibration with a time constant of 0.34 ps upon the 697 nm excitation in this study may suggest a previously unresolved anisotropy decay from the theoretical limit of the initial anisotropy of 0.4 to 0.3. With the current signal-to-noise ratio, the transient absorption in the Q_y region in this study is not showing a process corresponding to the 1.0 ps anisotropy change. The 1.0 ps component may thus represent energy transfer between Chls with similar absorption peaks around 686 nm, but with a significant difference in the molecular orientations. Although we cannot yet exactly tell which Chls are involved in each change, the biphasic energy equilibration (0.34 and 1.0 ps) upon the preferential excitation of P700 suggests an idea that at least two Chls or two excited states of Chls with PB/SE signal at around 686 nm are exchanging energy with P700*. On the other hand, our previous study on the transient absorption around 740 nm upon the excitation at 699 nm has shown a decaying component with a time constant of 0.1 ps,[19] which is attributable to a population decay of P700* and/or dephasing of the nuclear vibration of P700*. Because the previous time resolution (single wavelength method with an IRF of 0.12−0.15 ps) was better than that in this study, the true time constant for the spectral change in the Q_y region may also be shorter than 0.34 ps.

4.3. Vibrational Relaxation in Chlorophyll Molecules. In the case of the 653 nm excitation of Chl *a* in ethanol, there are two processes with time constants of 0.16 and 0.64 ps (Figure 6c). The first process causes a large increase in the area of the PB/SE signal around 670 nm. This represents the dissipation of the large excess vibrational energy between 653 nm and around 670 nm, because the absorption cross section around 670 nm is much larger than that at 653 nm. The second process with small amplitudes is a relaxation near the equilibrium of the vibrational energy distribution. A reverse process seems to proceed with a time constant of 1.1 ps upon the 677 nm excitation that inputs a relatively small excess vibrational energy into Chl *a* molecules (Figure 5b). It should be noted that the 0.64 ps DAS in the case of the 653 nm excitation seems to be a mirror image of the 1.1 ps DAS in the case of the 677 nm excitation (Figure 6, parts b and c). It should be also noted that the DASs for Chl *a* in ethanol may be affected in part by dynamic solvation effects as suggested in the case of Chl *b*.[30]

In view of the DAS upon the 653 nm excitation of Chl *a* in ethanol (Figure 6c), the 0.38 ps DAS in the case of the 662 nm excitation of P700-enriched RC should reflect the vibrational relaxation of individual Chls (Figure 3b). However, the negative component around 665 nm seems to be unique to Chls in the P700-enriched RC, because there is no equivalent component in the DAS of Chl *a* in ethanol upon the 653 nm excitation. It is thus concluded that 0.38 ps process of the P700-enriched RC upon the 662 nm excitation represents both vibrational relaxation and downhill energy transfer processes.

4.4. Residual Long-Wavelength-Absorbing Chlorophylls and Isolated Chlorophylls in the P700-Enriched RC. PSI RC core complex retaining about 100 chlorophylls/P700 usually contains the so-called long-wavelength-absorbing chlorophylls with absorption peaks redder than that of P700.[5,7,34−36] In the case of the P700-enriched RC, the shape of the transient absorption spectrum at 18 ps in the wavelength region of 695−

710 nm is not dependent on the excitation wavelength (Figure 2d). This result rules out any residual long-wavelength absorbing Chls from which energy transfer to P700 cannot be completed within 18 ps, because its PB/SE signal should be larger because of the direct optical excitation in the case of the excitation at 697 nm than in the case of the excitation at 662 nm. The amount of residual long-wavelength absorbing Chl in P700-enriched RC was previously estimated to be ≈0.1 molecules per P700 based on the spectral decomposition of steady-state absorption and fluorescence spectra.[21]

There is an extra PB/SE signal on the blue-wavelength side under the 662 nm excitation condition compared with under the 697 nm excitation condition (Figure 2d). The difference between the two spectra shows a peak at 676 nm (not shown). This is in good agreement with the report that there is at least one chlorophyll absorbing around 676 nm that is isolated from P700 in terms of energy transfer in the P700-enriched RC with 11 Chls/P700.[21] The ratio of the area of the extra PB/SE signal to the area of the total PB/SE signal at 0.3 ps upon the 662 nm excitation is 0.13. This indicates that the number of the isolated chlorophylls is at most 2 (≈16 × 0.13) in the P700-enriched RC with 16 Chls/P700.

4.5. Nature of Nonequilibrium Trapping in Intact PSI RC. Gobets et al. have recently reported streak-camera-based fluorescence-spectrum measurements, which have clearly indicated that the trapping of excitation energy (because of the primary charge separation) is biphasic in some cases of PSI RC retaining about 100 Chls/P700,[11,25] especially if the excitation wavelength is close to the peak of P700.[25] The fast phase of trapping, which is called nonequilibrium trapping, has a time constant of as short as 9.6 ps, and it is characterized by the fluorescence DAS with a peak between 688 and 700 nm.[5,11,25]

The nonequilibrium trapping component seems to be both kinetically and spectrally similar to the 7.2 ps phase of the primary charge separation in the case of 697 nm excitation of the P700-enriched RCs. The 7.2 ps DAS in this study probably corresponds to a fluorescence DAS peaking between 686 and 701 nm (see section 4.2). The delayed fluorescence of the P700-enriched RC that was thermally generated from $P700^+A_0^-$ actually shows a peak at 693 nm,[32] and it should be due to P700* and neighboring Chls excited by P700*. These similarities in both the spectrum as well as the time constant suggest that the nonequilibrium trapping component is observable when direct and/or indirect excitation of the Chls in the ETS results in the charge separation without considerable back energy transfer to the core antenna Chls in the case of intact PSI RC retaining about 100 Chls, as shown here in the case of P700-enriched RC.

4.6. Degree of Excitonic Coupling in the Electron-Transfer System. The earliest transient spectra at −0.1 ps in Figure 4 seems to represent a state consisting primarily of P700*, because the difference spectrum of $P700^+$/P700 shows the main peak at 696 nm.[14] The spectral change from −0.1 to +0.3 ps, together with the 0.34 ps DAS (Figure 3), suggests energy equilibration starting from P700* to more thermally equilibrated excited state of the ETS. However, this scenario may be in contrast to that suggested by Gibasiewicz et al., who studied PSI RC from *Chlamydomonas reinhardtii* CC 2696 at room temperature and 10 K with the help of transient absorption spectroscopy.[26,37] They found that the PB/SE signal at 0.16 ps shows a peak around 690 nm and a fwhm of about 25 nm upon the excitation centered at a wavelength longer than 700 nm with a fwhm of about 5 nm**.** This PB/SE signal was ascribed to exciton states because of the strongly interacting Chls (possibly over the 6 Chls) in the ETS,[37,38] which explains the unresolvably rapid appearance (<0.16 ps) of the wide PB/SE signal even at 10 K.

In the case of the 697 nm excitation of the P700-enriched RC, the initial PB/SE signal at −0.1 ps shows a peak at 696 nm, which means almost no blue shift compared with the excitation pulse (Figure 4). Despite the relatively wide fwhm of our excitation pulse (Figures 2a and 4), the spectral width of the PB/SE signal at −0.1 ps is 12 nm, which is twice narrower than the 0.16 ps spectra in ref 26. It should be noted that our IRF width seems to be similar to that in ref 26 and that our −0.1 ps seems to approximately correspond to the 0.16 ps in ref 26 because of the different definitions of the zero time.

The wide PB/SE spectrum that appears unresolvably fast in *Chlamydomonas reinhardtii* CC 2696 PSI in ref 26 is similar not to the −0.1 ps spectrum but rather to the 0.3 ps spectrum in the case of the 697 nm excitation in this study (Figure 4). The 0.3 ps spectrum results from the −0.1 ps spectrum with a resolvable time constant (0.34 ps or possibly shorter because of the IRF limitations) in this study. These may suggest that the excitonic interactions among the Chls in the ETS are somewhat weaker in the P700-enriched RC from spinach than in *Chlamydomonas reinhardtii* CC 2696.

5. Concluding Remarks

We have revealed the energy transfer processes among the Chls in the ETS with the help of tunable femtosecond laser and P700-enriched PSI RC. The blue-edge excitation (662 nm) of P700-enriched RC revealed a slow energy transfer from residual antenna Chls to P700, reverse process of which was not found in the case of the red-edge excitation (697 nm) of P700-enriched RC. Upon the red-edge excitation, there is an uphill energy transfer from the directly excited P700 to neighboring Chls absorbing around 686 nm in the ETS with a time constant of 0.34 ps.

Even upon the direct excitation of P700, there is a slow phase of the primary charge separation (7.2−9 ps, in Table 1) as well as the fast subpicosecond phase (0.8 ps).[19] The slow phase is attributable to the primary charge separation after equilibration of excitation energy among the Chls in the ETS. There are kinetic and spectral similarities between the slow phase of the primary charge separation in P700-enriched RC and the nonequilibrium trapping in PSI RC retaining about 100 Chls/P700. This suggests that the nonequilibrium trapping corresponds to the primary charge separation without considerable back energy transfer from the ETS Chls to the antenna Chls.

Acknowledgment. The authors thank Prof. S. Itoh for his valuable discussion. S.K. acknowledges supports from the Ministry of Education, Science, Sports and Culture of Japan (Nos. 10740320 and 14740379), the Simadzu Science Foundation, the Ogasawara Foundation for the Promotion of Science and Engineering, and the Inoue Foundation for Science.

References and Notes

(1) Nechushtai, R.; Eden, A.; Cohen, Y.; Klein, J. in *Oxygenic Photosynthesis: The Light Reactions*; Ort, D. R., Yocum, C. F., Eds.; Kluwer Academic Publishers: Dordrecht, The Netherlands, 1996; pp 289−311.

(2) Jordan, P.; Fromme, P.; Witt, H. T.; Klukas, O.; Saenger, W.; Krauβ, N. *Nature* **2001**, *411*, 909−917.

(3) Fromme, P.; Jordan, P.; Krauβ, N. *Biochim. Biophys. Acta* **2001**, *1507*, 5−31.

(4) Brettel, K. *Biochim. Biophys. Acta* **1997,** *1318*, 322−373.

(5) Gobets, B.; van Grondelle, R. *Biochim. Biophys. Acta* **2001**, *1507*, 80−99.

(6) Yoshihara, K.; Kumazaki, S. *J. Photochem. Photobiol. C* **2000**, *1*, 22−32.

(7) Karapetyan, N. V.; Holzwarth, A. R.; Rögner, M.*FEBS Lett.* **1999**, *460*, 395−400.

(8) Savikhin, S.; Xu, W.; Soukoulis, V.; Chitnis, P. R.; Struve, W. S. *Biphys. J.* **1999**, *76*, 3278−3288.

(9) Melkozernov, A. N.; Lin, S.; Blankenship, R. E. *Biochemistry* **2000**, *39*, 1489−1498.

(10) Kennis, J. T. M.; Gobets, B.; van Stokkum, I. H. M.; Dekker, J. P.; van Grondelle, R.; Fleming, G. R. *J. Phys. Chem. B* **2001**, *105*, 4485−4494.

(11) Gobets, B.; van Stokkum, I. H.; Rogner, M.; Kruip, J.; Schlodder, E.; Karapetyan, N. V.; Dekker, J. P.; van Grondelle, R. *Biophys. J.* **2001**, *81*, 407−424.

(12) Gibasiewicz, K.; Ramesh, V. M.; Lin, S.; Redding, K.; Woodbury, N. W.; Webber, A. N. In the Proceedings of the 12th International Congress on Photosynthesis; CSIRO Publishing: Australia (www.publish.csiro.au/ps2001).

(13) Ikegami, I.; Itoh, S.; Iwaki, M. *Plant Cell Physiol.* **1995**, *36*, 857−864.

(14) Ikegami, I.; Itoh, S.; Iwaki, M. *Plant Cell Physiol.* **2000**, *41*, 1085−1095.

(15) Kumazaki, S.; Kandori, H.; Petek, H.; Yoshihara K.; Ikegami, I. *J. Phys. Chem.* **1994**, *98*, 10335−10342.

(16) Kumazaki, S.; Iwaki, M.; Ikegami, I.; Kandori, H.; Yoshihara, K.; Itoh, S. *J. Phys. Chem.* **1994**, *98*, 11220−11225.

(17) Itoh, S.; Iwaki, M.; Ikegami, I. *Biochim. Biophys. Acta* **2001**, *1507*, 115−138.

(18) Iwaki, M.; Kumazaki, S.; Yoshihara, K.; Erabi, T.; Itoh, S. *J. Phys. Chem.* **1996**, *100*, 10802−10809.

(19) Kumazaki, S.; Ikegami, I.; Furusawa, H.; Yasuda, S.; Yoshihara, K. *J. Phys. Chem. B* **2001**, *105*, 1093−1099.

(20) Kumazaki, S.; Ikegami I.; Abiko, K.; Yasuda, S.; Yoshihara, K. to be published.

(21) Iwaki, M.; Mimuro, M.; Itoh, S. *Biochim. Biophys. Acta* **1992**, *1100*, 278−284.

(22) Kumazaki, S.; Furusawa, H.; Yoshihara, K.; Ikegami, I. In *Photosynthesis: Mechanism and Effects*; Garab, G., Ed.; Kluwer Academic Publishers: Dordrecht, The Netherlands, 1998; Vol. 1, pp 575−578.

(23) Ikegami, I.; Katoh, S. *Biochim. Biophys. Acta* **1975**, *376*, 588−592.

(24) Hastings, G.; Reed, L. J.; Lin, S.; Balnkenship, R. E. *Biophys. J.* **1995**, *69*, 2044−2055.

(25) Gobets, B.; Dekker, J. P.; van Grondelle, R. In *Photosynthesis: Mechanisms and Effects*; Garab, G, Ed.; Kluwer Academic Publisher: Dordrecht, The Netherlands, 1998; pp 503−508.

(26) Gibasiewicz, K.; Ramesh, V. M.; Melkozernov, A. N.; Lin, S.; Woodbury, N. W.; Blankenship, R. E.; Webber, A. N. *J. Phys. Chem. B* **2001**, *105*, 11498−11506.

(27) van Grondelle, R. *Biochim. Biophys. Acta* **1985**, *811*, 147−195.

(28) The time constant of the single step energy transfer between Chls in the electron-transfer system was tentatively estimated by the following equation: $(1/\tau) = C\tau_{rad}^{-1}n^{-4}\kappa^{-2}R^{-6}$ (Visser, M., Ph.D. Dissertation, Department of Physics and Astronomy, Vrije Universiteit, Netherlands, 1996), where τ is expressed in ps, C is a constant that incorporates the overlap integral of the absorption and fluorescence spectra of energy donor and acceptor, τ_{rad} is the time constant of the radiative decay, n is refractive index, κ is the orientation factor, and R is the center-to-center distance of molecules in nm. $C\tau_{rad}^{-1}$ is estimated to be 162 nm^6 ps^{-1} for a pair of Chl *a* molecules if the peak wavelengths of the absorption and fluorescence coincide and when τ_{rad} is assumed to be 15 ns (ref 29). The refractive index was assumed to be 2.0, and the κ and R were estimated by the Protein data bank file (1JB0). We have also confirmed that a computer simulation based on the above formula, parameters and crystal structure (our unpublished results) approximately reproduces the fastest decay (about 0.16 ps) of the polarization anisotropy of the fluorescence from photosystem I as observed in ref 10. Although all of the formula and parameters may not be very valid, we claim only that the time scales we have tentatively estimated as in Table 2 are reasonable.

(29) Palsson, L. O.; Spangfort, M. D.; Gulbinas, V.; Gillbro, T. *FEBS Lett.* **1994**, 339, 134−138.

(30) Oksanen, J. A. I.; Martinsson, P.; Akesson, E.; Hynninen, P. H.; Sundstrom, V. *J. Phys. Chem. A* **1998**, *102*, 4328−4336.

(31) Savikhin, S.; Xu, W.; Martinsson, P.; Chitnis, P. R.; Struve, W. S. *Biochemistry* **2001**, *40*, 9282−9290.

(32) Itoh, S.; Iwaki, M. *Biochim. Biophys. Acta* **1988**, *934*, 32−38.

(33) Kumazaki, S.; Ikegami, I.; Yoshihara K. *J. Phys. Chem. A* **1997**, *101*, 597−604.

(34) Pålsson, L.-O.; Flemming, C.; Gobets, B.; van Grondelle, R.; Dekker, J. P.; Schlodder, E. *Biphys. J.* **1998**, *74*, 2611−2622.

(35) Shubin, V. V.; Bezsmertnaya, I. N.; Karapetyan, N. V. *J. Photochem. Photobiol. B* **1995**, *30*, 153−160.

(36) Turconi, S.; Schweitzer; Holzwarth, A. R. *Photochem. Photobiol.* **1993**, *57*, 113−119.

(37) Gibasiewicz, K.; Ramesh, V. M.; Lin, S.; Woodbury, N. W.; Webber, A. N. *J. Phys. Chem. B* **2002**, *106*, 6322−6330.

(38) Beddard, G. S. *J. Phys. Chem. B* **1998**, *102*, 10966−10973.